Synoptics of dust intrusion days from the African continent into the Atlantic Ocean

J. Barkan,[1,2] H. Kutiel,[1] P. Alpert,[3] and P. Kishcha[3]

Received 4 December 2003; revised 18 February 2004; accepted 8 March 2004; published 16 April 2004.

[1] The phenomenon of dust intrusion from north Africa into the Atlantic Ocean was examined on daily bases for the month of July from 1983 to 1988 (184 cases). Composite patterns of wind flows and geopotential heights for the intrusion versus no-intrusion cases as well as the difference between them (intrusion minus no intrusion), in the area (60°W–25°E, 0°–60°N), were analyzed. For both intrusion and no-intrusion days a closed high pressure, centered at approximately (45°W, 32°N), was found, with a ridge northeastward. East of the ridge was a trough located to the west of the European and the north African coast. Further east was a closed high in the western Sahara with a ridge northeastward. Each of the maps presenting the difference between the two aforementioned variables shows two highs: one over western Europe and the other, quite strong, west of the African coast on the 24°N–25°N latitudes. Between them, centered about (15°W, 37°N), there is a low-pressure area. As a result of the higher pressure at the African anticyclone in the intrusion cases, an easterly-northeasterly flow dominates at the latitudes 18°N–22°N, which presumably causes the dust intrusion from the continent into the Atlantic. Correlation between the Total Ozone Mapping Spectrometer aerosol index on the one hand and the wind magnitude and the *u* and *v* components on the other hand was also analyzed for the entire data set. Correlation coefficients of $r = 0.52$, $r = -0.46$, and $r = -0.27$ were found. Analysis of two extreme intrusion and no-intrusion cases in July 1983 demonstrates the synoptic situation that allows the Saharan dust to reach England and NW Europe. *INDEX TERMS:* 0305 Atmospheric Composition and Structure: Aerosols and particles (0345, 4801); 3309 Meteorology and Atmospheric Dynamics: Climatology (1620); 3364 Meteorology and Atmospheric Dynamics: Synoptic-scale meteorology; *KEYWORDS:* Sahara, dust transport, dust intrusion

Citation: Barkan, J., H. Kutiel, P. Alpert, and P. Kishcha (2004), Synoptics of dust intrusion days from the African continent into the Atlantic Ocean, *J. Geophys. Res.*, *109*, D08201, doi:10.1029/2003JD004416.

1. Introduction

[2] The African continent, especially its northern part, is one of the main sources of dust around the globe. There are major source areas that emit huge quantities of dust into the atmosphere almost constantly, but more so in the summer months [*Prospero et al.*, 2002; *Dayan et al.*, 1991; *Dulac et al.*, 1996].

[3] Intrusion of this dust from the African continent and especially, from north and central Africa, into the tropical North Atlantic Ocean is a frequent phenomenon in the spring and summer months of the Northern Hemisphere. Strong heating of the Sahara and the Sahel regions in summer, causes strong convective disturbances, which elevate huge quantities of dust from the source regions at about 15°–20°N up to the 600–800-hPa levels [*Prospero*, 1996]. The deep warm low, formed because of this heating, causes a strong converging flow, especially from the northeast, called locally Harmatan. This flow adds to the already existing dust by uprooting dust particles and lifting them up [*Karyampudi et al.*, 1999]. Consequently, the atmosphere above north Africa is loaded with dust, available for transport according to the prevailing flow [*Israelevich et al.*, 2002]. Large quantities of this available dust are transported westward, toward the Atlantic Ocean with the easterly waves, which emerge from the African coast every 3–4 days [*Prospero*, 1996; *Westphal et al.*, 1987]. The dust is transported mainly above the humid trade wind air of the PBL in an uplifted turbulent Saharan air layer (SAL) while the dust is bounded within several distinct sub layers [*Carlson and Prospero*, 1972; *Hamonou et al.*, 1999; *Westphal et al.*, 1987]. The intrusions happen in a well-defined corridor of 10 degrees latitude width. This corridor moves from south to north and vice versa from 5°N in the early spring to 25°N in August, presumably connected with the movement of the ITCZ [*Swap et al.*, 1996; *Alpert et al.*, 1998]. In the tropical North Atlantic Ocean, at these altitudes, the main activity is in the summer months, especially in June and July [*Chiapello et al.*, 1997].

[1]Department of Geography, University of Haifa, Haifa, Israel.
[2]Now at Department of Geophysics and Planetary Sciences, Raymond and Beverly Sackler Faculty of Exact Sciences, Tel Aviv University, Tel Aviv, Israel.
[3]Department of Geophysics and Planetary Sciences, Raymond and Beverly Sackler Faculty of Exact Sciences, Tel Aviv University, Tel Aviv, Israel.

0148-0227/04/2003JD004416$09.00

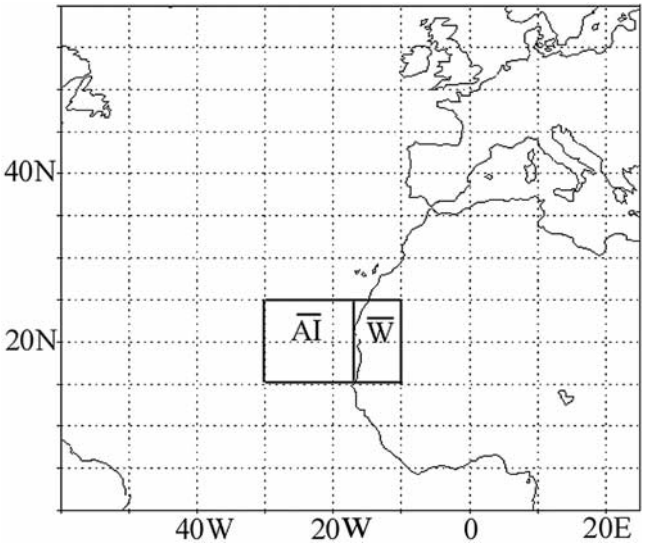

Figure 1. The research area for the synoptic analysis (60°W–25°E, 0°–60°N). The AI area represents the dust domain, while the W area represents the wind domain.

The main sources of the dust for these penetrations are the Spanish Sahara, Mauritania and Senegal [*Carlson and Prospero*, 1972; *Prospero et al.*, 1981; *Swap et al.*, 1996; *Chiapello et al.*, 1997]. Considerable differences were observed in the intensity of the intrusion activity from year to year. The intrusions happen in well-defined areas, but the point of any particular intrusion along the coast seems unpredictable. The duration is between 1–10 days, but moderate to severe intrusions last at least two days [*Swap et al.*, 1996]. In the summer months the African dust reaches the Caribbean and even the North American continent within a week, as a distinct air mass, different from the surrounding local air [*Prospero et al.*, 1981]. In winter, dust transport does exist, but at lower level within the trade wind layer (around the 850-hPa level) and the dust is deposited much closer to the African continent. The winter dust concentration in the air was observed and studied in the Cape Verde archipelago [*Chiapello et al.*, 1997].

[4] According to the latest Terra-MODIS observations (Y. Kaufman personal communication, 2004), the quantity of dust reaching the South American continent in winter is higher than was estimated by *Swap et al.* [1996]. Probably, the quantities of dust transported into North America in summer and South America in winter are quite close.

Table 1. Distribution of the Cases for July 1983–1988[a]

Year	Intrusion	Normal	No-Intrusion
1983[b]	8	11	10
1984	9	12	10
1985	9	12	10
1986	9	12	10
1987	11	9	11
1988	8	14	9
Total	54	70	60

[a]Here AI, 17°E–30°W/15°N–25°N; wind variables, 10°W–17°W/15°N–25°N.
[b]In 1983, only 29 days were available.

Table 2. Average Values and Standard Deviations (in Parentheses) of the Aerosol Index and the Wind Variables for Intrusion and No-Intrusion Cases in the W Box Area[a]

	AI	*u*, m/s	*v*, m/s	d, degree	Magnitude, m/s
Intrusion	3.42 (0.58)	−8.63 (2.75)	−2.57 (2.23)	17.5 (19.6)	9.33 (2.4)
No-intrusion	1.63 (0.45)	−4.88 (3.27)	−1.01 (2.08)	7.2 (30.1)	5.72 (2.64)

[a]See Figure 1.

[5] A number of studies were performed over the past four decades on the intrusion of dust from the African continent to the Atlantic Ocean and its transport across the ocean to the Americas. Various aspects of the phenomena were described, such as frequency, duration, vertical and horizontal extension, composition, source areas, etc. [*Prospero and Carlson*, 1972; *Swap et al.*, 1996; *Alpert et al.*, 2004].

[6] In the present study we aim at detecting and analyzing the differences in the synoptic situations between intrusion and no-intrusion cases. Understanding the synoptic situation will help model dust generation in GCMs. The understanding and describing of the synoptic situation can help models predict dust generation, with application to a wide range of topics like traffic safety, agriculture, marine biology, health problems etc. In addition, a better understanding of the synoptics associated with deep dust intrusion will help the forecasters to improve their predictions.

2. Methodology and Data Processing

[7] This work is based on data for the month of July from 1983 to 1988. The month of July was chosen due to the highest intrusion activity of dust from primary dust source areas into the tropical North Atlantic in this month [*Chiapello et al.*, 1997].

[8] Daily data of the wind components, geopotential heights and temperature at the 700-hPa level are from the NCEP/NCAR reanalysis. The aerosol index (AI) daily data are from the NASA database of the TOMS (Total Ozone Mapping Spectrometer) measurements. The 700 hPa level was chosen because the average transportation of the dust takes place above the humid trade wind air of the PBL, between 600–800 hPa [*Carlson and Prospero*, 1972; *Prospero*, 1996; *Hamonou et al.*, 1999; *Alpert et al.*, 2004; *Westphal et al.*, 1987].

[9] The research area for the synoptic analysis is (60°W–25°E, 0°–60°N). The average AI data was computed for the area (30°W–17°W, 16°N–26°N). The average atmospheric variables (*u* wind component, *v* wind component and wind magnitude) were computed for the area (10°W–17°W, 16°N–26°N). Shown in Figure 1, the "AI" area represents the fluctuation of the dust quantity as function of the synoptic parameters, while the "W" area represents the wind that drives the dust. The "W" domain was chosen because it includes the most active sources in the summer season: Mauritania and the western Sahara [*Chiapello et al.*, 1997; *Israelevich et al.*, 2002]. The "AI" domain was chosen because it is due west to the "W" domain and the dominant winds being primarily easterlies or at least with a considerably easterly component, it is the most likely area to

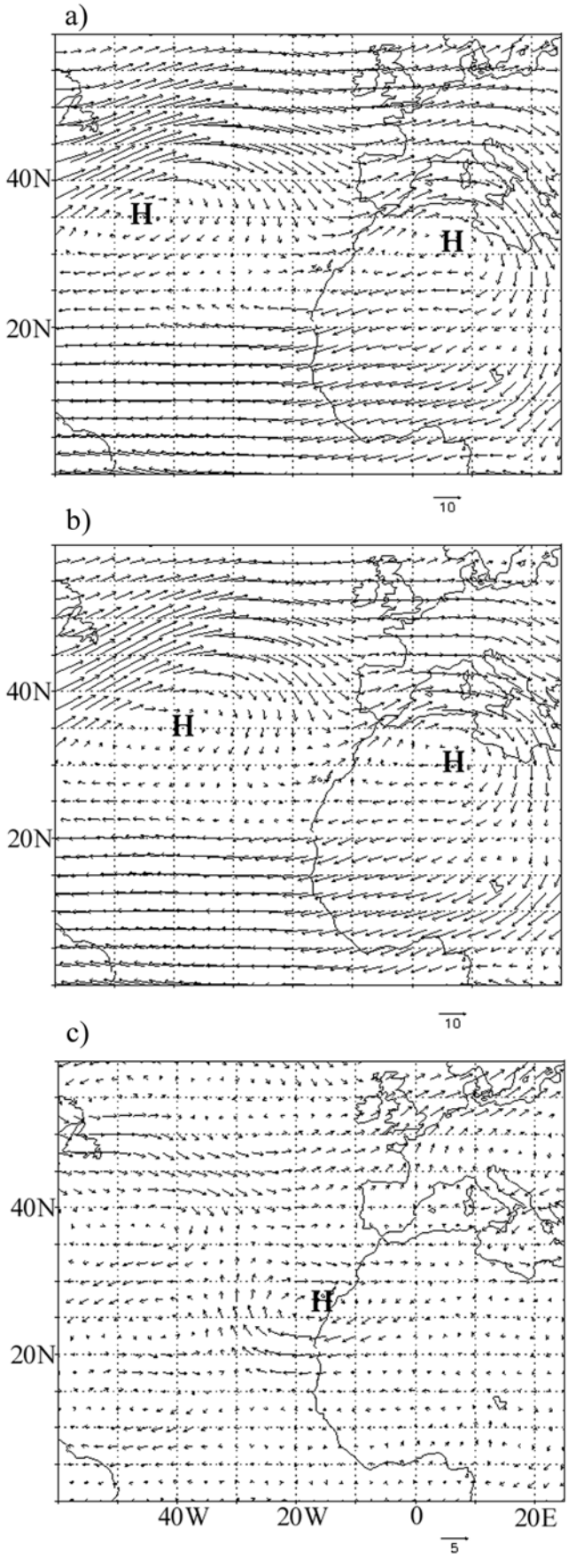

find the major portion of the dust which was driven out into the Atlantic.

[10] In the current study the daily TOMS-AI values were standardized for each year in the period 1983–1988. Standardization (known also as Normalization) is a procedure in which the mean of series is reduced to 0 and its standard deviation to 1. This is achieved by subtracting the mean of the series from each of its components and dividing the difference by its standard deviation. The obtained values of the standardized AI are dimensionless. Negative standard scores indicate below average values, whereas positive scores, above average. The intrusion and the no-intrusion case thresholds were defined by ±0.5 standard deviation. Days in which standardized AI scores were $\geq$0.5 were defined as intrusion cases, whereas days in which standardized AI scores were ≤ -0.5 were defined as no-intrusion cases. Days with values between these two thresholds were defined as normal. This threshold of ±0.5 was selected in order to obtain a fairly large sample of days defined either as intrusion or no-intrusion cases. One standard deviation would have left us with too few cases of intrusion/no-intrusion to allow a significant result. The distribution of the cases by year and the total is shown in Table 1. According to this definition, based on the raw data, +0.5 equal to AI = 2.93 and −0.5 equal to AI = 2.07. These values of TOMS AI correspond to dust load (DL) from 1.03 to 1.47 g/m^2 in accordance with the approximate expression 0.5 $AI \cong DL$ by *Alpert et al.* [2002].

[11] The average values of the AI and wind variables of all the 184 cases were computed for the intrusion and the no-intrusion cases as shown in Table 2. One can see clear distinction between the intrusion and the no-intrusion cases. The average values of AI, u and v wind components and wind magnitude are almost twice in the intrusion cases as compared to the ones in the no-intrusion cases. The average wind direction in the intrusion cases was more to the east than in the no-intrusion cases.

3. Results and Discussion

3.1. Wind Flow

[12] In Figure 2a (intrusion cases) we see a closed high in the western edge of the research area centered, approximately, at (40°W, 35°N). Along the western shores of the Iberian Peninsula and Morocco a weak trough can be observed. East of the southern part of the trough there is a closed high in the western Sahara. In the southern flank of this high a considerable easterly-northeasterly flow can be found, especially in the vicinity of the western African coast, around latitude 25°N.

[13] The most important differences between the intrusion and no-intrusion cases (Figure 2b) are that the trough west of the European and African coasts penetrates further south and, consequently, the flow in the western Saharan and the

Figure 2. (a) Average wind flow of the intrusion cases at 700 hPa, July 1983–1988. (b) Average wind flow of the no-intrusion cases at 700 hPa, July 1983–1988. (c) Average wind flow difference, i.e., intrusion minus the no-intrusion cases over the study region, July 1983–1988.

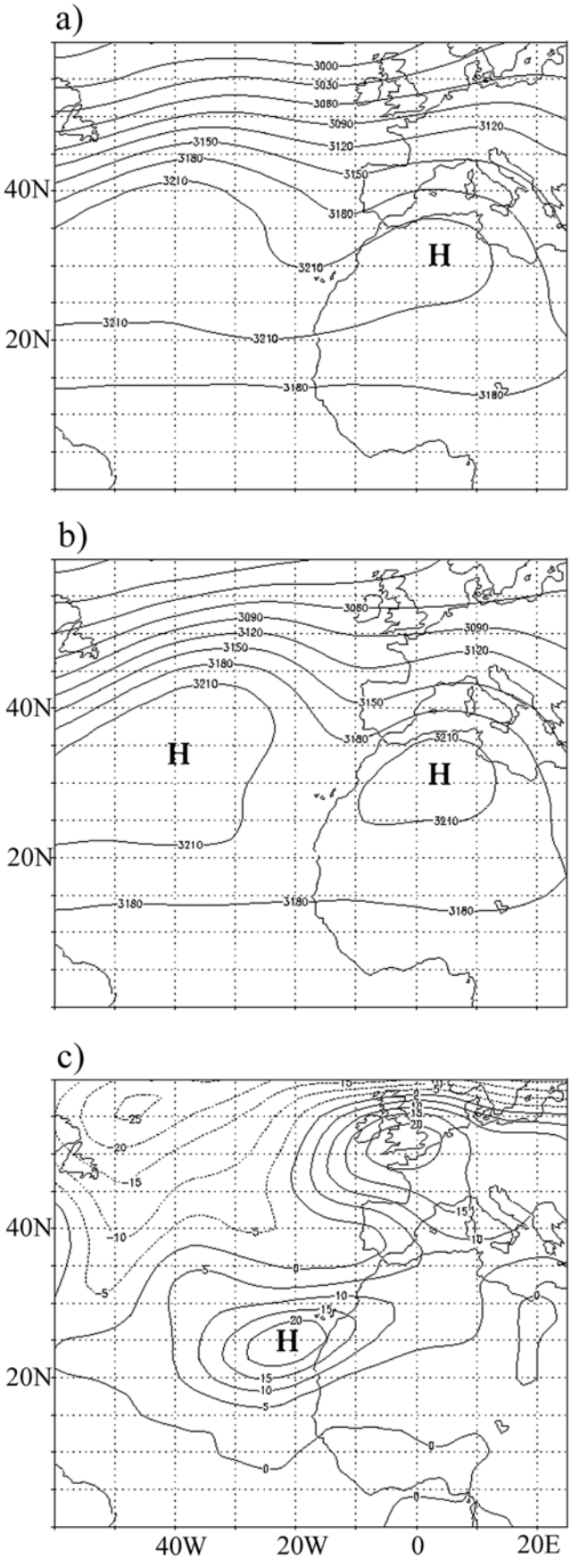

Moroccan coast is more southwesterly and weaker. The significant differences are illustrated next. The wind vector difference between intrusion and no-intrusion (Figure 2c), shows a strong and well-defined anticyclone near the Mauritanian coast, at 22°W–23°N. On its eastern flank the difference vector is northeasterly, of quite considerable strength. Further to the east, the difference vector is easterly northeasterly, though weaker. At the southern flank of the anticyclone, in the Atlantic, the difference vector is easterly reaching about longitude 40°W where it turns north and westward. This relative change in the flow structure strongly suggests enhanced transportation of dust from the mean dust source areas into the Atlantic, in intrusion days, i.e., 0.5 σ above the monthly average of TOMS-AI. Since the vector difference actually shows the real additional flow [*Stidd*, 1956] the dust transport toward and into the Atlantic in these cases seems reasonable.

[14] To obtain an additional view of the synoptic variation, the geopotential heights at the 700-hPa level were compared in the intrusion and the no-intrusion cases. In the intrusion cases (Figure 3a) there is a weak ridge within the westerly flow around the 35W-30W longitudes. Consequently, the trough to the east along the European and north African coast is shallow, especially in the south. The 3210 m isohyet passes north of the Canary Islands. The subtropical high is continuous from the west into the Sahara. In the no-intrusion cases (Figure 3b), on the other hand, the trough west of the European and African continents penetrates considerably south and actually cuts the subtropical high into two sections. There is a closed high in the Sahara, somewhat weaker than in the intrusion cases. The difference between the intrusion and no-intrusion cases (Figure 3c) shows a closed high of 25 m in its center west of the western Saharan coast. In its eastern and southern flanks there are northeasterly and easterly flows, respectively. There is a closed −25 m low at 48°W–56°N, a trough due south and another one, although weak, due east. The latter separates the abovementioned high from another one in southern England. This construction can hint at the cause of the two highs and the resulting flow.

3.2. Correlation

[15] The correlations between the AI and the various wind variables at 700 hPa were computed for all the 184 cases (including the normal cases) and scatter diagrams prepared. The correlation between the AI and the magnitude of the wind is 0.52 (Figure 4a). A positive correlation means, that the stronger the wind over the land the more dust penetrates the Ocean, as was expected. More interestingly, however, is the correlation between the AI and the *u* component of the wind (Figure 4b), which is also sufficiently high, −0.46. This negative correlation suggests a link between the AI and the easterly component of wind. On the other hand the correlation between the *v* component and the AI (Figure 4c) is considerably lower, −0.27 (the

Figure 3. (a) Average geopotential height of the intrusion cases at 700 hPa, July 1983–1988. (b) Average geopotential height of the no-intrusion cases at 700 hPa, July 1983–1988. (c) Average geopotential height difference, intrusion minus no-intrusion cases, July 1983–1988.

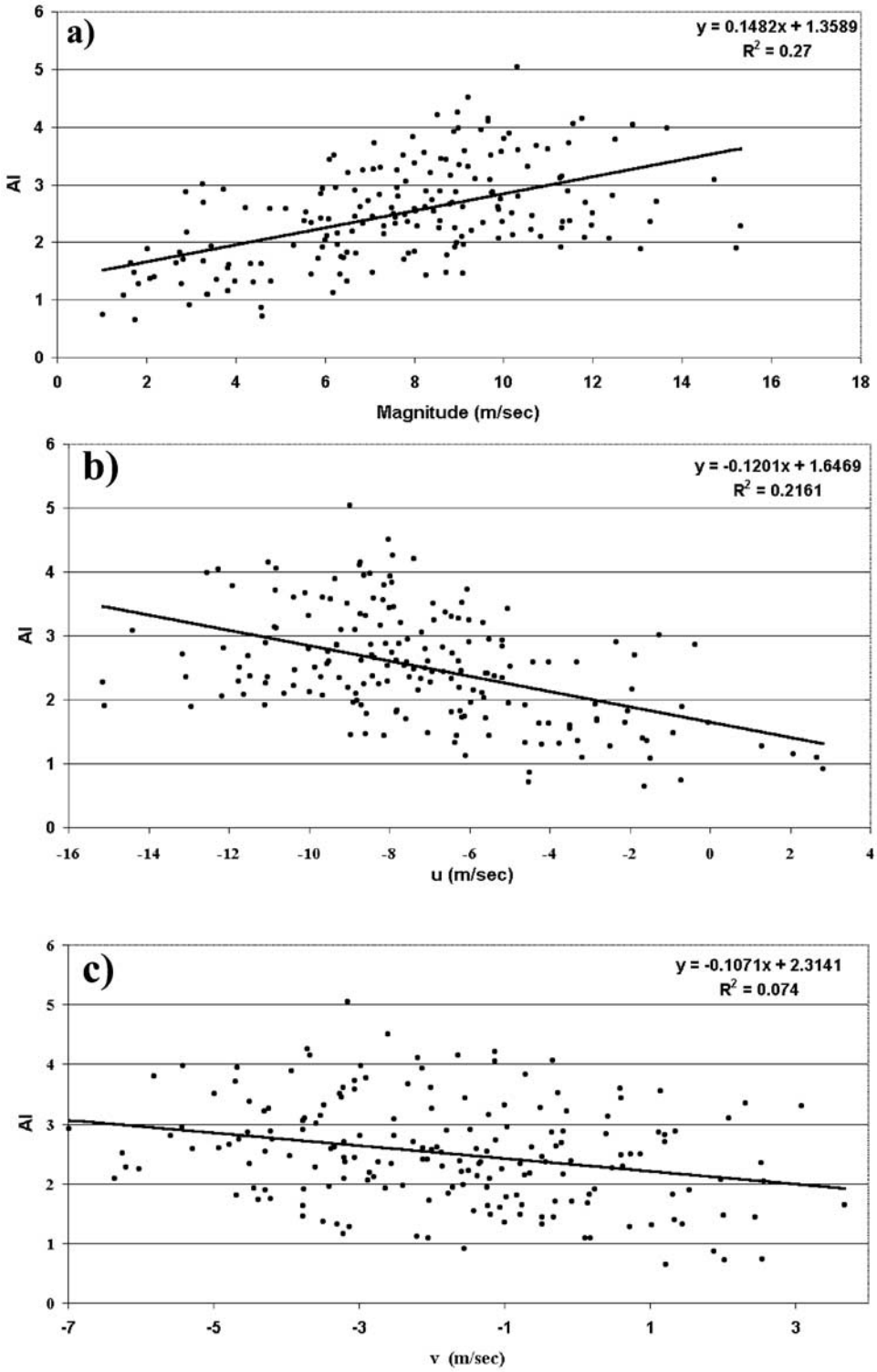

Figure 4. (a) Scatterplot between the magnitude of the wind at 17°W, 10°W–15°N, 25°N and the aerosol index at 30°W, 17°W–15°N, 25°N, July 1983–1988, 700 hPa, $r = 0.52$. (b) Scatterplot between the u component of the wind at 17°W, 10°W–15°N, 25°N and the aerosol index at 30°W, 17°W–15°N, 25°N, July 1983–1988, 700 hPa, $r = -0.46$. (c) Scatterplot between the v component of the wind at 17°W, 10°W–15°N, 25°N and the aerosol index at 30°W, 17°W–15°N, 25°N, July 1983–1988, 700 hPa, $r = -0.27$.

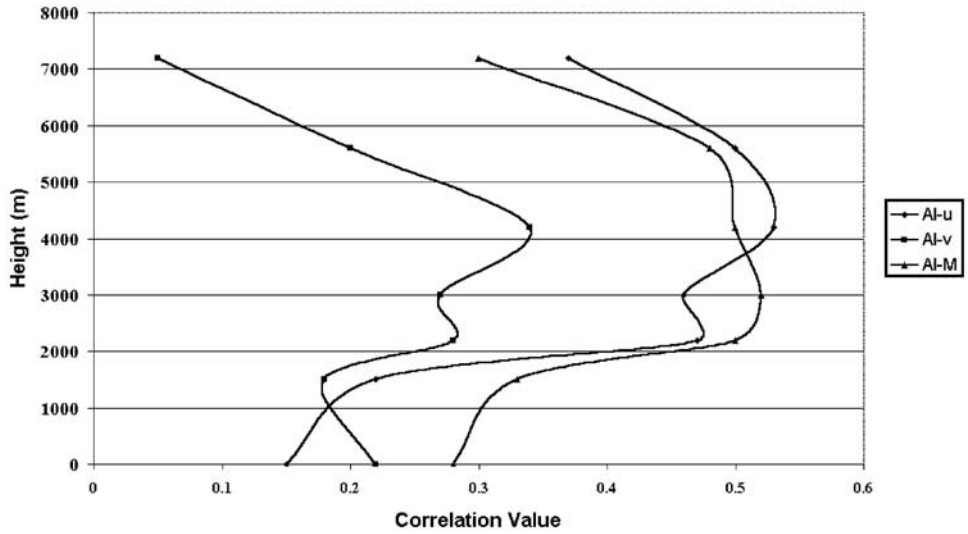

Figure 5. Vertical profiles of correlation between the aerosol index and the wind variables at several heights. Since for dust below 1 km TOMS-AI values are less reliable, values there are in doubt.

definition of the meridian component is from south to north). The consequence is that strong easterly winds transport dust toward the Atlantic more efficiently. Keeping in mind that the most violent dust intrusions occur between latitudes 18N–25N, the most active dust sources in July are in Mauritania almost exactly to the east of this section of the shore.

[16] Concerning the correlation between the magnitude of the wind and the AI we wanted to test the assumption that the correlation with the kinetic energy of the wind (W^2) will be higher. Actually it was lower (0.44). We think that the reason is as follows: the kinetic energy of the flow is indeed the main factor in the vicinity of the source areas. But the target area (the AI domain) is far from the dust sources. Therefore the quantity of the dust in it depends on the advection, which is a function of the wind magnitude.

[17] Some indication on the thickness of the dust layer may be obtained from the vertical profiles of the calculated correlations shown in Figure 5 where u is the west-east component of the wind, v is the south-north component of the wind, M is the magnitude of the wind and AI the aerosol index. The correlation between the u component, the magnitude and the AI is rather high between 2000 and 6000 m but almost nonexistent at the lower levels and considerably less above 6000 m. This suggests that the mean dust layer is approximately between these heights. These results are in accordance with the vertical distribution of the Atlantic dust layer described in the literature [*Carlson and Prospero*, 1972; *Prospero*, 1996; *Chiapello et al.*, 1997; *Hamonou et al.*, 1999; *Alpert et al.*, 2004].

3.3. Extreme Case Studies: 16–19 and 25–28 July 1983

[18] During 16–19 July 1983 the standardized AI data showed values considerably higher than 0.5, i.e., there was a continuous and strong intrusion of dust during these four days. On the contrary, in the period 25–28 July 1983 the AI data showed values considerably lower than 0.5, i.e., there was no intrusion of dust at all during these 3 days.

[19] Next, average 700 hPa maps for wind flow and geopotential height in these periods and the difference between them in the research area were analyzed. In the intrusion period the wind flow map (Figure 6a) was similar to the average intrusion map (Figure 2a) but with stronger easterly northeasterly flow between the 20–25N meridians in the vicinity of the African coast. There is a clearly defined ridge emanating from the western part of the subtropical high toward the northeast, i.e., along the NW African coast and into Italy. On the contrary, there is a strong closed low west to the European coast, instead of a trough, as in the average case. The subtropical high penetrates eastward into Africa and almost unites with the closed high on the Mediterranean coast of Algeria. At the eastern and southern flanks of these two highs a strong northeasterly to easterly flow exists and is clearly transports the dust from the source areas into the Atlantic.

[20] The wind flow map for the no-intrusion period (Figure 6b) is perhaps the key to understanding the dynamics behind this phenomenon. The western center of the subtropical high is further to the south and the east of the same center in the intrusion period (Figure 6a). Instead of the ridge in the intrusion period (Figure 6a), there is a strong closed high, with its center at 30°W–44°N. This high is completely cut off from the subtropical high. East of this high there is a closed low just like in the intrusion period (Figure 6a) further east, its center over the Iberian Peninsula. But its most relevant feature is a trough emanating from it and strongly penetrating southwest, reaching approximately latitude 22°N. Consequently there is a strong southwesterly flow from latitude 20°N across western Sahara, Mauritania and Algeria toward the Mediterranean. East to the Iberian low is the eastern section of the subtropical high as a closed high cut off from its western part, which is much stronger than the high in the intrusion period (Figure 6a) and centered further north in the western

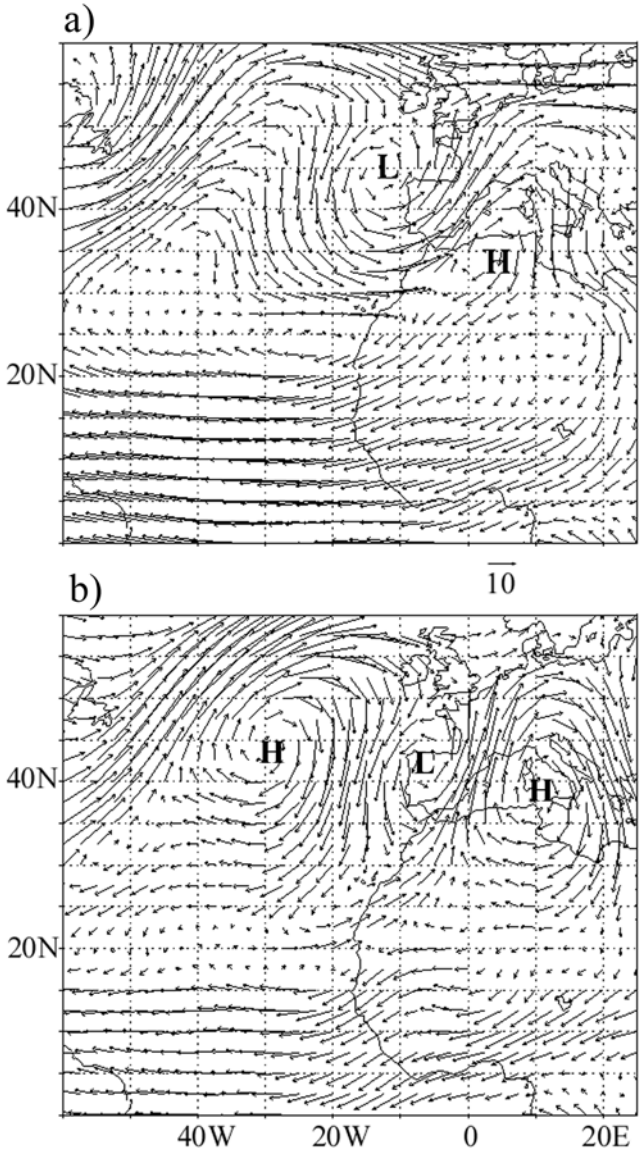

Figure 6. (a) Average wind flow of the intrusion period at 700 hPa, 16–19 July 1983. (b) Average wind flow of the no-intrusion period at 700 hPa, 25–28 July 1983.

Mediterranean between Sardinia and Sicilia. The flow in its southern flank is easterly but it weakens rapidly toward the south and does not reach the Atlantic coast at the critical section for dust transport between 20°N–25°N.

[21] The map of the wind flow difference between the intrusion and the no-intrusion period (Figure 7a) demonstrates the dynamics of the intrusion process in extreme cases. The high-latitude (40°N–55°N) eastern Atlantic is dominated by a strong closed low. South to it is the subtropical high composed of two cells approximately along latitude 25°N. The eastern cell just west of the western Saharan coast is stronger, and a ridge emanates from it to the northeast toward western Europe. This structure is associated with a strong westerly flow between the Atlantic low and the eastern cell of the subtropical high, the southwesterly flow in its northern section, and most relevant to our case, very strong northeasterly and easterly flow at the eastern and southern flank of the eastern cell. The wind vector difference between the two periods is as high as 15 m/s (compared to 6 m/s in Figure 2c) and provides, in our opinion, quite a satisfactory explanation to the dust intrusion phenomenon. These strong easterlies continue along the southern flank of the Subtropical high reaching 55°W. It is interesting that at longitude 30°W–35°W the flow splits up. Part of it turns to the north along the western flank of the eastern cell of the subtropical high. This flow then turns back to the east together with the strong westerlies between this cell and the deep low in the midlatitude eastern Atlantic. It is suggested here that in such extreme cases, when enormous quantities of dust are transported into the tropical Atlantic and the flow is strong; part of the dust reaches the

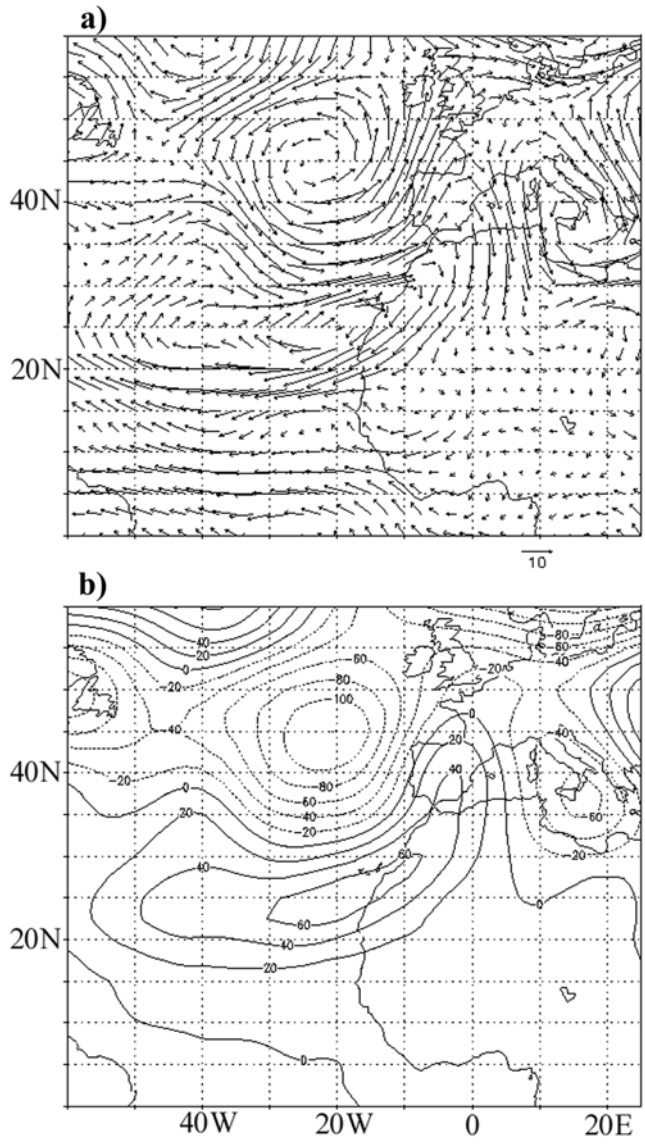

Figure 7. (a) Average wind flow difference, i.e., intrusion period 16–19 July 1983 minus no-intrusion period 25–28 July 1983, over the study region. (b) Average geopotential height difference, i.e., intrusion period 16–19 July 1983 minus no-intrusion period 25–28 July 1983, over the study region.

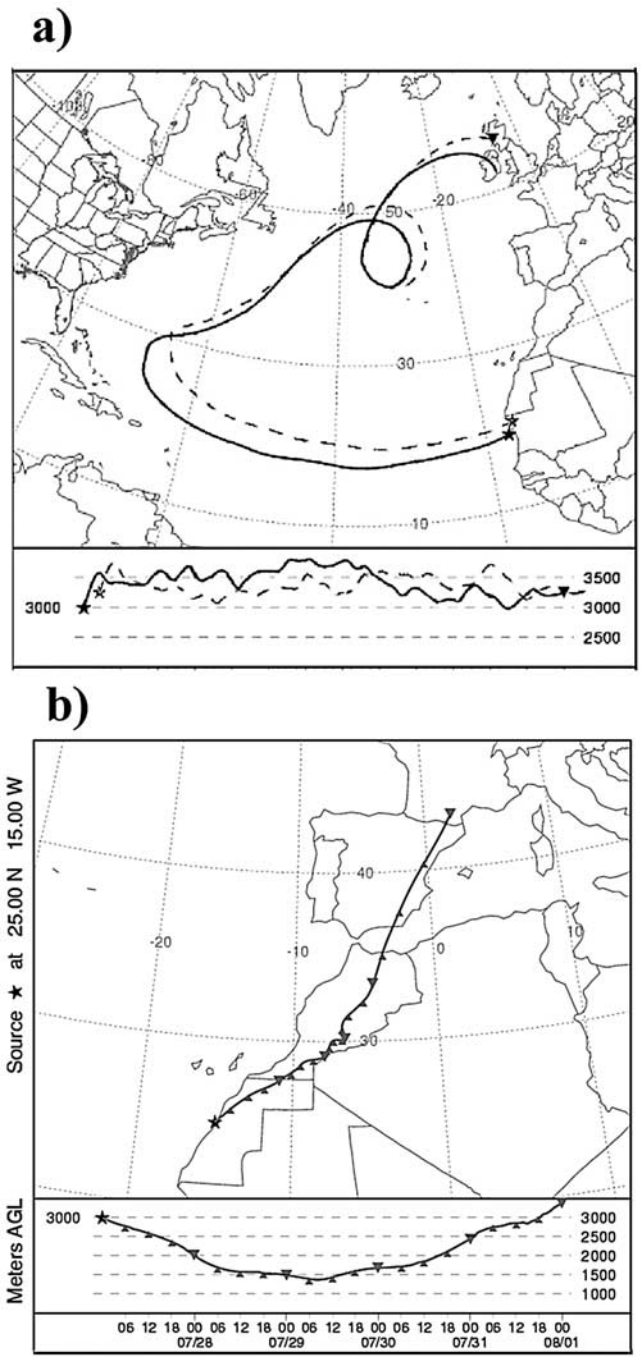

Figure 8. (a) Forward trajectories, 16–28 July 1983. Starting point 18°N, 17°W (full line), 19°N, 17°W (dashed line). Starting height 3000 m. (b) Forward trajectory, 27–30 July 1983. Starting point 25°N, 15°W.

American continent and another part is transported back toward Europe. To check this assumption, we computed the trajectory of an air parcel starting from the African coast on 16 July 1983, using the NOAA ARL HYSPLIT model. Figure 8a shows that in 13 days the air parcel (and presumably the dust) reaches the British Islands. The height of the air parcel along the route, which was computed also by the model, did not change much from its original altitude of 3000 m (approximately 700 hPa) height. Consequently we may assume, that part of the dust, which was not deposited along the long track, reached the same destination.

[22] Trajectories that were computed in other dates with less intrusion activity went some distance westward then turned back to the northeast. In the no-intrusion case, trajectory that started at 27 July 1983 turned immediately to the northeast and did not reach the Atlantic at all (Figure 8b).

[23] Figure 6b is the geopotential height difference between the extreme intrusion and no-intrusion cases. Actually it provides a similar but smoother picture to the flow difference in Figure 6a. There is a positive difference of more then 60 m coinciding with the center of the anticyclonic flow near the western Saharan coast and a negative difference of 100 m coinciding with the strong cyclonic flow in the eastern north Atlantic.

4. Conclusions

[24] TOMS-AI data from an area in the Atlantic (17°W–30°W, 15°N–25°N) west of the African coast and wind data at the 700-hPa level from an area (10°W–17°W, 15°N–25°N) inland, for the July months from 1983 to 1988 were extracted and classified as intrusion, normal or no-intrusion cases. The differences in the synoptic situations between the intrusion and the no-intrusion cases were explored, employing average wind flow and geopotential height, in the area (60°W–25°E, 0°–60°N). Maps of the difference between the intrusion and no-intrusion cases were also analyzed. A case study, based on the same technique as in the average cases, was carried out for a strong and continuous intrusion period of four days, versus a three day period with no-intrusion activity. In addition correlations between the AI and the wind variables for all the cases were examined.

[25] The most significant difference between the intrusion and no-intrusion cases is the deep south penetration of the trough west of Europe into the north African coast in the no-intrusion cases; while in the intrusion cases the trough line is terminated further north at about 34°N. The result is, that in the intrusion cases, a continuous high pressure belt from the west Atlantic into the Sahara region (i.e., stronger subtropical high) causes a westerly flow over the western Mediterranean and an easterly to northeasterly flow in the southern Sahara, toward the Atlantic coast around latitude 25°N. This happens to be the primary area of the intrusion occurrences in the summer months. On the other hand, in the no-intrusion cases, the southward penetration of the trough splits the subtropical high into two sections, causing on the western African coast and its vicinity a very weak flow (about 2–3 m/s) with a marked southern component. This flow significantly reduces the possibility of dust intrusion from Africa into the Atlantic.

[26] A case study of two extreme cases, one of a strong intrusion period of four days and the other one for a three-day period without intrusion, provides nearly similar synoptic patterns to the average cases, but greatly enhanced. In particular, it illuminates the difference between the no-intrusion and the intrusion periods. In the former, the deep southward penetration of the trough along the African coast causes a southwesterly flow as far as latitude 20°N and practically prevents dust intrusion from the continent into the Atlantic. In the intrusion period the midlatitude eastern

Atlantic low is deep but the penetration of the trough is terminated in the south by a strong westerly flow between latitudes 30°N–35°N. As a result, there is a closed subtropical high cell, the westerly flow forming its northern flank and the north easterly and easterly backflow toward the Atlantic enables the transport of dust westward far into the sea. Computations of the trajectories in both cases verify this picture.

[27] Correlations between the aerosol index over the sea and the wind variables over the land (see map) were computed. The correlations between AI and the wind magnitude and its west-east u component maximize at about the 700 hPa level with the values of; $r = -0.52$ and $r = -0.46$ respectively. The correlation with the v component is considerably lower, $r = -0.27$. Hence, as expected, strong winds with a large easterly component are the most efficient in transporting dust from the African continent into the Atlantic.

[28] **Acknowledgments.** The study was supported by the EU DETECT Project (contract EVK2-CT-1999-00048) and also by a grant (GLOWA–Jordan River) from the Israeli Ministry of Science and Technology and the German Bundesministerium fuer Bildung und Forschung (BMBF).

References

Alpert, P., Y. J. Kaufman, Y. Shai-El, D. Tanre, A. da-Silva, S. Schubert, and J. H. Joseph (1998), Quantification of dust forced heating of the lower troposphere, *Nature*, *395*, 364–370.

Alpert, P., S. O. Krichak, M. Tsidulko, H. Shapir, and H. Joseph (2002), A dust prediction system with TOMS initialization, *Mon. Weather Rev.*, *130*(9), 2335–2345.

Alpert, P., P. Kischa, A. Shtivelman, S. O. Krichak, and J. H. Joseph (2004), Vertical distribution of Saharan dust based on 2.5-year model predictions, *Atmos. Res.*, in press.

Carlson, T. N., and J. M. Prospero (1972), The large scale movement of Saharan air outbreaks over the northern equatorial Atlantic, *J. Appl. Meteorol.*, *11*, 283–297.

Chiapello, I., G. Bergametti, B. Chatenet, P. Bosquet, F. Dulac, and E. Santos Soares (1997), Origins of African dust transported over the southeastern tropical Atlantic, *J. Geophys. Res.*, *102*(D12), 13,701–13,709.

Dayan, U., J. Hefter, J. Miller, and G. Gutman (1991), Dust intrusion events into the Mediterranean basin, *J. Appl. Meteorol.*, *30*, 1185–1199.

Dulac, F., C. Moulin, C. E. Lambert, F. Guillard, J. Poitou, W. Guelle, C. R. Quetel, X. Schneider, and U. Ezal (1996), Quantitative remote sensing of African dust transport to the Mediterranean, in *The Impact of Desert Dust Across the Mediterranean*, edited by S. Guerzoni and R. Chester, pp. 25–49, Kluwer Acad., Norwell, Mass.

Hamonou, E., P. Chazette, D. Bali, F. Dulac, X. Schneider, F. Galani, G. Ancellet, and A. Papayannis (1999), Characterization of the vertical structure of the Saharan dust export to the Mediterranean Basin, *J. Geophys. Res.*, *104*(D22), 256–270.

Israelevich, P. L., Z. Levin, J. H. Joseph, and E. Ganor (2002), Desert aerosol transport in the Mediterranean region as inferred from the TOMS aerosol index, *J. Geophys. Res.*, *107*(D21), 4572, doi:10.1029/2001JD002011.

Karyampudi, M. V., et al. (1999), Validation of the Saharan dust plume conceptual model using lidar, Meteosat and ECMWF data, *Bull. Am. Meteorol. Soc.*, *80*(6), 1045–1076.

Prospero, J. M. (1996), Saharan dust transport over the North Atlantic Ocean and the Mediterranean, in *The Impact of Desert Dust Across the Mediterranean*, edited by S. Guerzoni and R. Chester, p. 133–151, Kluwer Acad., Norwell, Mass.

Prospero, J. M., and T. N. Carlson (1972), Vertical and aerial distribution of Saharan dust over the western equatorial North Atlantic Ocean, *J. Geophys. Res.*, *77*, 5255–5265.

Prospero, J. M., R. A. Glaccum, and R. T. Nees (1981), Atmospheric transport of soil dust from Africa to South America, *Nature*, *289*, 570–572.

Prospero, J. M., P. Ginoux, O. Torres, S. E. Nicholson, and T. E. Gill (2002), Environmental characterization of global sources of atmospheric soil dust identified with the NIMBUS 7 Total Ozone Mapping Spectrometer (TOMS) absorbing aerosol product, *Rev. Geophys.*, *40*(1), 1002, doi:10.1029/2000RG000095.

Stidd, C. K. (1956), The use of correlation fields in relating precipitation in circulation, *J. Meteorol.*, *11*, 202–213.

Swap, R., S. Waushi, M. Cobbet, and M. Gornstag (1996), Temporal and spatial characteristics of Saharan dust, *J. Geophys. Res.*, *101*(D2), 4205–4220.

Westphal, D. L., O. B. Toon, and T. N. Carlson (1987), A two dimensional numerical investigation of the dynamics and microphysics of Saharan dust storms, *J. Geophys. Res.*, *92*(D3), 3027–3049.

P. Alpert, J. Barkan, and P. Kishcha, Department of Geophysics and Planetary Sciences, Faculty of Exact Sciences, Tel-Aviv University, Ramat Aviv, Tel-Aviv 69978, Israel. (yossib@vortex.tau.ac.il)

H. Kutiel, Department of Geography, University of Haifa, Haifa 31905, Israel. (kutiel@geo.haifa.ac.il)